Multiwavelength observation from radio through very-high-energy γ-ray of OJ 287 during the 12-year cycle flare in 2007

Masaaki Hayashida[*], Giacomo Bonnoli[†], Antonio Stamerra[†], Elina Lindfors[‡], Kari Nilsson[‡] and Masahiro Teshima[§] for the MAGIC collaboration and Hiromi Seta[¶], Naoki Isobe[‖], Makoto S. Tashiro[¶], Koichiro Nakanishi[**], Mahito Sasada[††], Yoshito Shimajiri[‡‡] and Makoto Uemura[x]**

[*]*Kavli Institute for Particle Astrophysics and Cosmology, SLAC National Accelerator Laboratory, CA, 94025, USA*
[†]*Università di Siena, and INFN Pisa, I-53100 Siena, Italy*
[‡]*Tuorla Observatory, University of Turku, FI-21500 Piikkiö, Finland*
[§]*Max-Planck-Institut für Physik, D-80805 München, Germany*
[¶]*Department of Physics, Saitama University, Saitama 338-8570, Japan*
[‖]*Department of Astronomy, Kyoto University, Kyoto 606-8502, Japan*
[**]*Nobeyama Radio Observatory, Nagano 384-1305, Japan*
[††]*Department of Physical Science, Hiroshima University, Higashi-Hiroshima 739-8526, Japan*
[‡‡]*Department of Astronomy School of Science, University of Tokyo, Tokyo 113-0033, Japan*
[x]*Astrophysical Science Center, Hiroshima University, Higashi-Hiroshima 739-8526, Japan*

***Abstract*. We performed simultaneous multiwavelength observations of OJ 287 with the Nobeyama Millimeter Array for radio, the KANATA telescope and the KVA telescope for optical, the Suzaku satellite for X-ray and the MAGIC telescope for very high energy (VHE) γ-ray in 2007. The observations were conducted for a quiescent state in April and in a flaring state in November-December. We clearly observed increase of fluxes from radio to X-ray bands during the flaring state while MAGIC could not detect significant VHE γ-ray emission from the source. We could derive an upper limit (95% confidence level) of 1.7% of the Crab Nebula flux above 150 GeV from about 41.2 hours of the MAGIC observation. A simple SSC model suggests that the observed flaring activity could be caused by evolutions in the distribution of the electron population rather than changes of the magnetic field strength or Doppler beaming factor in the jet.**

***Keywords*: Blazar OJ 287 Multiwavelength observation**

I. Introduction

OJ 287 ($z = 0.306$ [22]) is one of the archetypal and most studied blazars. An outstanding characteristic of the object is its recurrent optical outbursts with a period of 11.65 years, as revealed by optical data spanning more than 100 years [23]. "The OJ 94 project" [25] confirmed the periodicity and revealed that the optical outbursts consist of two peaks corresponding to flares with an interval of about one year [24]. OJ 287 is suggested to be a binary black hole system in which a secondary black hole pierces the accretion disk of the primary black hole and produces two impact flashes per period [29]. The differences between the two flares may be interpreted as following; the first flare have a thermal origin in the vicinity of the black hole and the accretion disk while the second one originate from synchrotron radiation from the jet [31]. However, we have not yet obtained any convincing evidence supporting this interpretation.

The multiwavelength spectral energy distribution (SED) has the potential to resolve the physical state of OJ 287 during the flares. In general, the SED of blazars is characterized by two broad humps (e.g., [6]); the low-energy component, with wavelengths in the range between radio to ultraviolet and X-ray, is widely regarded as synchrotron radiation from relativistic electrons within the jet. The high-energy component, with wavelengths in the range between X-rays and γ-rays, is interpreted as inverse-Compton (IC) scattering. In one of the simple emission models, named "synchrotron self-Compton (SSC) model", relativistic electrons scatter synchrotron photons produced by the same population of electrons (e.g., [8]). For low-frequency peaked BL Lac objects (LBLs), a class of blazars to which OJ 287 belongs, the synchrotron peak is located in the range between sub-mm and optical wavelengths [17]. IC scattering in LBLs can emit radiation up to very-high-energy (VHE: E>50 GeV) γ-rays during their optical high states; VHE γ-ray emission has been detected, for example, from BL Lacertae [2] and S5 0716+714 [27]. These two components usually intersect with each other in the X-ray band (e.g., [9]).

In the period between 2005 and 2008, OJ 287 was predicted to move to the last active phase, and was in fact reported to exhibit the first optical outburst in 2005 November [29], [30]. Since the second flare of the source was expected to be in the fall of 2007 ([28],

[14]), we organized two simultaneous multiwavelength observation campaigns from radio through VHE γ-ray, in the quiescent state in April 2007 (MWL I) between the two outbursts and in the second flaring state in November-December 2007 (MWL II), with the objective to reveal the characteristics of the second flare, in comparison with the quiescent state.

In this contribution, we present the results of the multiwavelength campaigns with detailed observation results of the VHE γ-ray band by MAGIC, and discuss the overall SEDs using a SSC model. More extensive discussions of the campaigns including detailed results of the Suzaku X-ray satellite and other wavelength observations can be found in [21].

II. Multiwavelength Observations and Results

A. VHE γ-ray band by MAGIC

We used the MAGIC telescope to search for VHE γ-rays emission from OJ 287 during the both MWL campaigns. MAGIC is a single dish Imaging Atmospheric Cherenkov Telescope with a 17-m diameter main reflector. The telescope is located in the Canary Island of La Palma, in regular operation since 2004 with a low energy threshold of 50 – 60 GeV (trigger threshold at small zenith angles; [3]).

In MWL I, MAGIC observed the source during 3 nights. The zenith angle of the observations ranges from 8° to 29°. The observations were performed in so-called ON-OFF observation mode. The telescope was pointing directly to the source, recording ON-data. The background was estimated from additional observations of regions where no γ-ray is expected, OFF-data, which were taken with sky conditions similar to ON-data. Data runs with anomalous trigger rates due to bad observation conditions were rejected from the analysis. The remaining data correspond to 4.5 hours of ON and 6.5 hours of OFF data. In November and December 2007 for MWL II, MAGIC observed in a zenith angle range from 8° to 31° in the "wobble mode" [7], where the object was observed at 0.4° offset from the camera center. In this observation mode, an ON-data sample and OFF-data samples can be extracted from the same observation run; in our case, we used 3 OFF regions to estimate the background. In total, the data were taken during 22 nights. 41.2 hours of data from 19 nights passed the quality selection to be used for further analysis.

The VHE γ-ray data taken for MWLs I and II were analyzed using the MAGIC standard calibration and analysis software. Detailed information about the analysis chain is found in [3]. In February 2007, the signal digitization of MAGIC was upgraded to 2 $\mathrm{GSamples\ s^{-1}}$ FADCs, and timing information is used to suppress the contamination of light of the night sky and to obtain new shower image parameters [5] in addition to conventional *Hillas* image parameters [10].

These parameters were used for γ/hadron separation by means of the "Random Forest (RF)" method [4]. The γ/hadron separation based on the RF method was tuned to give a γ-cut efficiency of 70 %. Finally, the γ-ray signal was determined by comparing between ON and normalized-OFF data in the —ALPHA— parameter[1] distribution, in which the γ-ray signal should show up as an excess at small values. Our analysis requires a γ-cut efficiency of 80 % for the final —ALPHA— selection. The energy of the γ-ray events are also estimated using the RF method.

A search of VHE γ-rays from OJ 287 was performed with data taken for MWLs I and II in three distinct energy bins. No significant excess was found in any data samples. Upper limits with 95 % confidence level in the number of excess events were calculated using the method of [19], taking into account a systematic error of 30 %. The number of excess events was converted into flux upper limits assuming a photon index of -2.6, corresponding to the value used in our Monte-Carlo samples of γ-rays. The derived upper limits in the three energy bins for each period are summarized in table I.

A search for VHE flares with a short-time scale was also performed with the data taken for MWL II. Figure 1 shows the nightly count rate of the excess events after all cuts including a SIZE cut above 200 photoelectrons, corresponding to an energy threshold of 150 GeV. Fitting a constant to the observed flux yields $\chi^2/\mathrm{d.o.f.} = 25.55/18$ (a probability of 11 %), and thus indicating no evidence of a VHE flare during this period.

TABLE I: Results of the search for VHE γ-ray emissions from OJ 287.

MWL I			
Threshed Energy[1]	80	145	310
ON events[2]	40056	1219	42
OFF events[3]	40397 ± 226	1340 ± 38	39.5 ± 6.3
significance (σ)[4]	-1.13	-0.94	-0.47
U.L. of excess[5]	394	75.1	21.9
$\mathrm{Flux_{95\%U.L.}}$[6]	59.8	11.1	2.83
Crab Flux(%)[7]	8.5	3.3	2.4
MWL II			
Threshed Energy[1]	85	150	325
ON events[2]	281885	12582	578
OFF events[3]	282342 ± 493	12573 ± 65	576 ± 14
significance (σ)[4]	-0.75	0.07	0.07
U.L. of excess[5]	1218	330	71.6
$\mathrm{Flux_{95\%U.L.}}$[6]	22.1	5.64	1.18
Crab Flux(%)[7]	3.4	1.7	1.1

[1] in [GeV]. Corresponding to peak energies of γ-ray MC samples after all cuts. [2] Number of measured ON events. [3] Normalized number of OFF events and related error. [4] Based on equation (17) in [15]. [5] 95% upper limit of the number of excess events with 30% systematic error. [6] in $[\times 10^{-12}\ \mathrm{cm^{-2}\ s^{-1}}]$. Flux upper limit assuming a photon index of -2.6 for the calculation of the effective area. [7] Corresponding Crab flux in each energy range based on measurements of the Crab pulsar performed with the MAGIC telescope [3].

B. Other energy bands

In the X-ray band, the Suzaku satellite [16] observed OJ 287 in the quiescent state (MWL I) between 19:47:00

[1] the angle between the shower image principal axis and the line connecting the image center of gravity with the camera center.

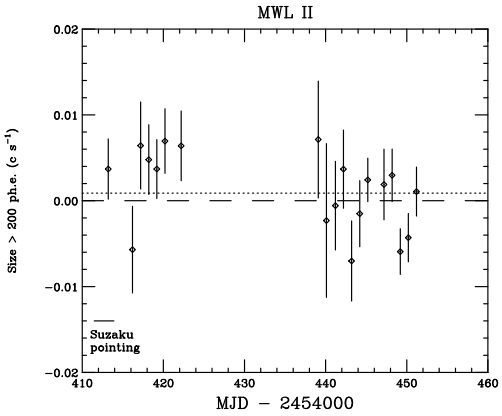

Fig. 1: Excess event rate with SIZE above 200 photoelectrons (with a corresponding energy threshold of 150 GeV), observed with the MAGIC telescope in MWL II. The dotted line indicates the average count rate.

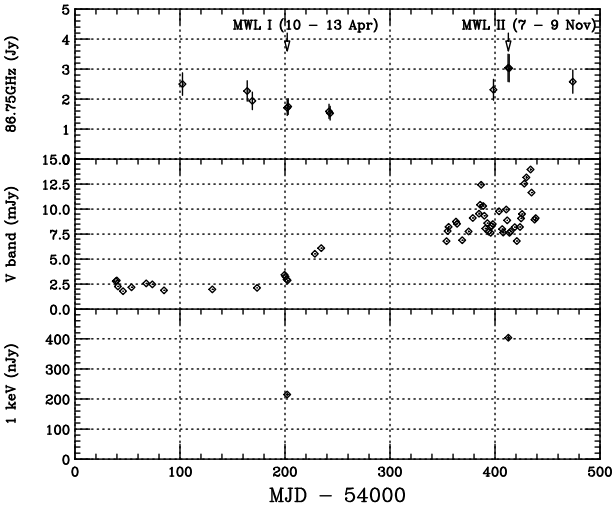

Fig. 2: The multiwavelength lightcurves of OJ 287. The top panel shows the radio flux at 86.75 GHz as observed with NMA, while the middle panel shows the optical flux in the V-band as observed with KANATA. The radio and optical fluxes are averaged over each night. The bottom panel shows the X-ray flux density at 1 keV. Arrows indicate the Suzaku pointings in MWL I and MWL II.

UT 2007 April 10 and 11:10:19 UT April 13, and the second flare (MWL II) between 11:24:00 UT 2007 November 7 and 21:30:23 UT November 9. Significant X-ray signals were detected in the 0.5 – 10 keV range in both observations. Hard X-ray signals in 12 – 27 keV was also clearly detected with a significance of 5.0 σ in MWL II while those signals were not significant in MWL I.

Optical flux was monitored by the KANATA telescope in Hiroshima, Japan (in V, J, and K_s-bands), and the KVA telescope in the Canary Island of La Palma (in R-band). Radio continuum emission from OJ 287 at 86.75 GHz and 98.75 GHz was also observed with the Nobeyama Millimeter Array (NMA) in Nobeyama, Japan.

Figure 2 summarizes the multiwavelength lightcurves of the radio, optical (V) and X-ray bands obtained between September 2006 and January 2008. While the optical flux of OJ 287 was below 3 mJy in the V-band before MWL I, the brightness of the source started increasing after MWL I to become the flaring state (> 7 mJy) in September 2007. The optical data show a monotonous decrease in a time scale of ~ 4 days during MWL II by a factor of 1.3. The radio flux was generally higher during the optical flare in MWL II than in MWL I. The X-ray flux in MWL II also increased by a factor of 2 compared to the flux in MWL I. Table II shows the flux of each energy bands during the Suzaku pointing in both MWLs I and II.

III. Discussion

Figure 3 shows the overall SED of OJ 287 obtained during the MWL I and MWL II, as well as some historical data. The low frequency synchrotron component has a spectral turnover at around 5×10^{14} Hz. The X-ray spectrum exceeds the extrapolation from the optical synchrotron spectra in both observations. Therefore, we naturally attribute the observed X-ray spectra to the IC component rising toward the higher frequency range. The SED indicates that both the synchrotron and IC intensities increased from MWL I to MWL II without any significant shift of the synchrotron peak frequency.

As a working hypothesis, here we assume simply that the variation of the SED was caused by a change in electron energy density (or number density) and/or the maximum Lorentz factor of the electrons, with stable magnetic field, volume of emission region, minimum Lorentz factor, and break of electron energy distribution (e.g., [26]). In order to evaluate this hypothesis, we applied a one-zone SSC model to the SED by using the numerical code developed by [13]. The electron number density spectrum was assumed to be a broken-power law and the index of the electron spectrum (p) below the break Lorentz factor was determined by the X-ray photon index as $p = 2\Gamma - 1 = 2.3$ and 2.0, in MWL I and MWL II, respectively. We obtained the following seven free parameters to describe the observed SED: the Doppler factor (δ), the electron energy density ($u_{\rm e}$), the magnetic field (B), the blob radius (R), and the minimum, break, and maximum Lorentz factor of the electrons ($\gamma_{\rm min}$, $\gamma_{\rm break}$, and $\gamma_{\rm max}$, respectively). Adopting the optical variability time scale ($T_{\rm var} \sim 4$ days) in MWL II, the relation between δ and R should be subjected to $R < cT_{\rm var}\delta/(1+z) = 1.2 \times 10^{17}(T_{\rm var}/4{\rm days})(\delta/15)$ [cm] where c and z are the speed of light and the redshift of the source, respectively. We could reproduce SEDs in both MWL I and II by the SSC model as parameters are summarized in table III. The differences between two states can be found in p, $u_{\rm e}$ and $\gamma_{\rm max}$ while the other parameters remained unchanged. Thus, we conclude that the increase in the

TABLE II: Radio, optical and X-ray fluxes obtained during the Suzaku pointing in MWL I and MWL II.

obs	radio flux (Jy)		optical flux (mJy)				X-ray flux (nJy)	
	86.95 GHz[1]	98.75 GHz[1]	K_s [2]	J [2]	R [3]	V[2]	$S_{1\mathrm{keV}}$[4]	Γ[5]
MWL I	1.73 ± 0.26	1.75 ± 0.26	17.74 ± 0.33	8.82 ± 0.03	3.20 ± 0.05	3.03 ± 0.01	215 ± 5	1.65 ± 0.02
MWL II	3.04 ± 0.46	2.98 ± 0.46	$55.95^{+7.69}_{-6.76}$	27.02 ± 0.21	8.70 ± 0.14	8.93 ± 0.05	404^{+6}_{-5}	1.50 ± 0.01

[1] NMA data. [2] KANATA data. [3] KVA data. [4] flux density at 1 keV of Suzaku data. [5] photon index of the Suzaku data (0.5-10 keV).

electron energy density produced the second flare.

In 2008, Fermi Gamma-ray Space Telescope successfully detected a γ-ray spectrum from the quiescent state of OJ 287 during its first three months [1], as shown in figure 3. The measured γ-ray flux significantly exceeds our simple SSC model flux. This may indicate a contribution of external Compton radiation to the γ-ray emission from OJ 287. A simultaneous multiwavelength observation with Fermi will be essential to test emission models with the external Compton radiation to the γ-ray component.

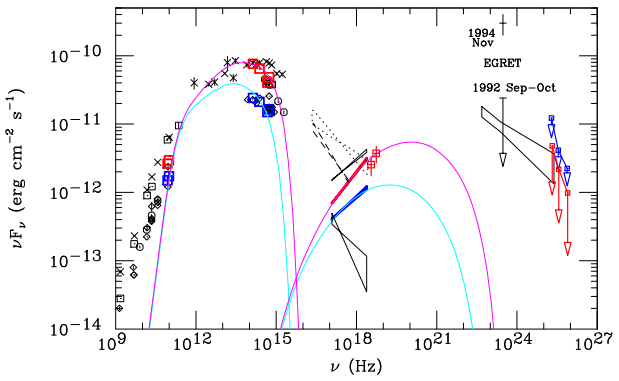

Fig. 3: The SED of OJ 287 during the Suzaku observations in MWL I (blue) and MWL II (red). The radio and optical data are shown with squares and, the X-ray data are shown with bow ties. The upper limit of the VHE γ-ray spectrum are measured values, shown with downward arrows. The light blue lines and the purple lines indicate the simple one-zone SSC model for MWL I and MWL II, respectively. The black data points show radio, optical, and γ-ray data from non-simultaneous observations. The X-ray spectra with EXOSAT, ROSAT, and ASCA are drawn with dotted, dashed, and solid lines, respectively ([11], [12] and references therein). The γ-ray spectrum obtained with Fermi during the first 3 month observation (August – October 2008) is shown with a bow tie [1]. The γ-ray emission can be attributed to the external Compton radiation.

TABLE III: Physical parameters for the SSC model.

parameters[1]	MWL I	MWL II
δ	15	
R (cm)	7.0×10^{16}	
B (Gauss)	0.71	
γ_{min}	70	
γ_{break}	700	
γ_{max}	3300	4500
p	2.3	2.0
u_{m} (erg cm^{-3})	2.0×10^{-2}	2.0×10^{-2}
u_{e} (erg cm^{-3})	1.5×10^{-3}	2.1×10^{-3}

[1] Notations are described in the text.

ACKNOWLEDGMENT

We would like to thank the Instituto de Astrofisica de Canarias for the excellent working conditions at the Observatorio del Roque de los Muchachos in La Palma. The support of the German BMBF and MPG, the Italian INFN and Spanish MICINN is gratefully acknowledged. This work was also supported by ETH Research Grant TH 34/043, by the Polish MNiSzW Grant N N203 390834, and by the YIP of the Helmholtz Gemeinschaft. We also thank all members of the Suzaku team for performing successful operation and calibration. The Nobeyama Radio Observatory is a branch of the National Astronomical Observatory of Japan, the National Institutes of Natural Sciences (NINS). IRAF is distributed by the National Optical Astronomy Observatories, which are operated by the Association of Universities for Research in Astronomy, Inc., under a cooperative agreement with the National Science Foundation.

REFERENCES

[1] Abdo, A. A., et al. 2009, arXiv:0902.1559
[2] Albert, J., et al. 2007, *ApJ*, 666, L17
[3] Albert, J., et al. 2008a, *ApJ*, 674, 1037
[4] Albert, J., et al. 2008b, Nucl. Instrum. and Meth., A588, 424
[5] Aliu, E., et al. 2009, Astroparticle Physics, 30, 293
[6] Fossati, G., et al., *MNRAS*, 299, 433
[7] Fomin, V. P., et al., 1994, Astropart. Phys., 2, 137
[8] Ghisellini, G., et al., 1998, *MNRAS*, 301, 451
[9] Giommi, P., et al., 1999, *A&A*, 351, 59
[10] Hillas, A. M. 1985, Proc. 29th Int. Cosmic Ray Conf. (La Jolla), 3, 445
[11] Idesawa, E., et al. 1997, *PASJ*, 49, 631
[12] Isobe, N., Tashiro, M., Sugiho, M., & Makishima, K. 2001, *PASJ*, 53, 79
[13] Kataoka, J., Ph.D thesis, 2000, Univ. of Tokyo
[14] Kidger, M. R. 2000, *AJ*, 119, 2053
[15] Li, T.-P., & Ma, Y.-Q. 1983, *ApJ*, 272, 317
[16] Mitsuda, K., et al. 2007, *PASJ*, 59, 1
[17] Padovani, P. & Giommi, P. 1995, *ApJ*, 444, 567
[18] Pursimo, T., et al. 2000, *A&AS*, 146, 141
[19] Rolke, W. A., López, A. M., & Conrad, J. 2005, Nucl. Instrum. and Meth., A551, 493
[20] Shrader, C.R., Hartman, R.C., Webb, J.R., 1996, *A&A*, 120, 599,
[21] Seta, H., et al. 2009, *PASJ*, submitted
[22] Stickel, M., Fried, J. W., & Kuehr, H. 1989, *A&AS*, 80, 103
[23] Sillanpää, A., et al. 1988, *ApJ*, 325, 628
[24] Sillanpää, A., et al. 1996, *A&A*, 315, L13
[25] Sillanpää, A., et al. 1996, *A&A*, 305, L17
[26] Takahashi, T., et al. 2000, *ApJ*, 542, L105
[27] Teshima, M., et al. 2008, The Astronomer's Telegram, #1500
[28] Valtonen, M. J., et al. 2006, *ApJ*, 643, L9
[29] Valtonen, M., et al., 2008, Nature, 452, 7189, 851
[30] Valtonen, M., et al., 2008, *A&A*, 477, 407
[31] Valtaoja, E., et al., 2000, *ApJ*, 531, 744
[32] Majumdar, P., et al. 2005, in Proc. 29th Int. Cosmic Ray Conf. (Pune, India), 5, 203